

---

# One-Step Distillation of Discrete Diffusion Image Generators via Fixed-Point Iteration

---

Chaoyang Wang Yunhai Tong  
Peking University  
cywang@stu.pku.edu.cn



Figure 1: Text-to-image samples from MaskGen-L distilled with our Fixed-Point Distillation (FPD) framework, where each image is synthesized in a single forward pass.

## Abstract

Discrete diffusion models excel at visual synthesis but rely on slow, iterative decoding. Existing single-step distillation methods attempt to bypass this bottleneck, either by training auxiliary score networks that effectively double compute, or by introducing specialized parameterizations and multi-stage pipelines that fragment optimization. In this paper, we introduce Fixed-Point Distillation (FPD), an end-to-end framework that constructs local correction targets by partially corrupting the student’s one-step draft and refining it with a single teacher step. To compute the training objective in a semantically meaningful space, we lift discrete tokens into continuous features and apply a multi-bandwidth drift loss that iteratively accumulates these corrections. To backpropagate through the discrete bottleneck, we employ a straight-through estimator that feeds exact hard-sampled tokens to the teacher and decoder during the forward pass, ensuring that training and inference operate on the same codebook manifold, while routing continuous gradients back to the student logits. This fully differentiable pathway additionally accommodates an optional unconditional adversarial objective to enhance perceptual realism. Evaluations on both class- and text-conditional generation validate the effectiveness of our framework. FPD achieves competitive visual fidelity and structural alignment within a single inference step, narrowing the gap to multi-step teachers while outperforming existing discrete distillation baselines.

# 1 Introduction

Generative models based on iterative refinement have emerged as the leading paradigm for high-fidelity visual synthesis. By breaking down the generative process into a sequence of transitional steps, these models accurately capture complex data distributions, driving rapid progress across text-to-image generation [38, 37, 39, 35, 40, 34], video synthesis [50, 20, 54, 21], image editing [6, 33], 3D asset creation [36], and world modeling [1, 7]. Among them, discrete diffusion models that operate on quantized token sequences have attracted growing attention for their natural compatibility with language-based architectures and scalable training. However, these methods typically share a fundamental computational bottleneck: the requirement for tens or hundreds of sequential network evaluations per sample. This high inference latency severely restricts their utility in latency-sensitive environments, motivating an intensive search for efficient acceleration methods.

An effective remedy is *distillation*, which trains a student model to reproduce the output of a pretrained teacher in far fewer steps. In the continuous domain, the literature has largely converged around three successful paradigms: trajectory imitation [43, 51, 30, 29, 14], distribution matching [56, 55, 31, 59], and adversarial post-training [45, 44]. These approaches now routinely yield robust one- to four-step generators. In contrast, the distillation of discrete masked diffusion models has advanced far more slowly. Existing discrete distillers generally follow one of two suboptimal paths. They either adapt the continuous score-distillation recipe by relying on an online auxiliary network [60, 61], which drastically inflates training compute and memory, or introduce correlation-aware objectives through bespoke designs — a mixture-model student parameterization [17] or multi-stage coupling rectification [57] — that bypass the auxiliary network but inflate per-step computation or fragment training into iterative offline stages. Neither route yields a single-step discrete distiller that is simultaneously efficient to train and universally applicable across different masking schedules. To overcome these limitations, we step away from artificial trajectory tracking and auxiliary surrogate score networks altogether, proposing a fundamentally different distillation paradigm.

In this work, we propose a principled, end-to-end distillation framework that fundamentally casts single-step generation as a fixed-point matching problem. **Our core motivation is to repurpose the frozen teacher as a state-dependent local refinement operator, rather than regressing toward pre-collected multi-step teacher rollouts.** Given a pretrained multi-step teacher, our method trains the student exclusively on its own generated drafts. Specifically, starting from a nearly fully masked token sequence with random codebook entries, the student produces a complete draft in a single forward pass. This draft is then partially re-masked and refined by the teacher through a single denoising correction, yielding a target tightly coupled to the student’s current output. At convergence, the student’s output distribution becomes invariant under this corruption-and-refinement cycle, meaning that single-step generation constitutes a fixed point of the distillation process. To compute the training objective in a meaningful metric space, we lift both the student’s draft and the teacher’s refinement into a shared continuous feature space via a frozen encoder. Since discrete tokens admit no well-defined distance, this lifted space allows us to apply a multi-bandwidth drift loss that provides stable gradient signals without auxiliary score networks. As training progresses, these local corrections accumulate, gradually steering the student’s generation toward the data manifold.

However, backpropagating the drift loss through the discrete sampling step is nontrivial. Conventional continuous relaxations, such as soft probability mixtures over codebook embeddings, produce off-manifold inputs that distort both the teacher’s refinement and the decoder’s reconstruction, introducing persistent bias in the training target. To resolve this, we employ a straight-through estimator (STE) that feeds exact hard-sampled tokens in the forward pass, ensuring that the decoder always receives valid discrete inputs, while routing continuous gradients from the drift loss back to the student logits during the backward pass. This ensures that training and inference operate on identical discrete inputs, eliminating the train-test mismatch inherent in soft relaxations. Moreover, the fully differentiable pathway from pixel space to logits additionally accommodates an optional unconditional adversarial loss on the decoded student images, which enhances perceptual realism without sacrificing the semantic alignment enforced by the drift objective.

Our contributions are summarized as follows: **1)** We propose Fixed-Point Distillation, a framework that formulates single-step discrete distillation as a fixed-point matching problem, bypassing complex trajectory tracking, pre-collected multi-step teacher samples, auxiliary score networks, or fragmented training pipelines. **2)** We introduce a lifted drift objective paired with a straight-through estimator, enabling fully end-to-end training through the discrete bottleneck with consistent training and infer-

ence behavior. 3) Empirical experiments and ablations verify the effectiveness, whilst demonstrating competitive performance against existing discrete distillation methods.

## 2 Related Work

### 2.1 Discrete Diffusion Models

Diffusion models learn to generate data by progressively corrupting it with a forward noising process and training a network to reverse the corruption. The continuous-domain lineage, spanning from early denoising models [19, 52] to modern flow matching architectures, has produced the dominant large-scale visual generators [13, 39, 35]. A parallel discrete branch works on quantized token sequences and forms the primary focus of this work. In the language domain, masked diffusion and score-entropy formulations [41, 28] implement absorbing- and uniform-state corruption processes, demonstrating generation capabilities that rival those of traditional autoregressive (AR) decoders at comparable scales. For visual synthesis, a growing line of work extends discrete diffusion to image generation [2, 8, 48, 5, 16, 23, 53]. Among them, masked generative transformers such as MaskGIT [9] and MaskGen [24] iteratively predict and reveal tokens over a fixed schedule, differing primarily in their tokenization strategies and conditioning mechanisms. Regardless of these design choices, discrete diffusion models typically require tens to hundreds of sequential forward passes per sample, severely limiting their deployment in latency-sensitive settings.

### 2.2 Discrete Diffusion Distillation

While continuous-domain distillation has matured rapidly through trajectory imitation [43, 51, 29, 14], distribution matching [56, 55], and adversarial frameworks [45, 44], the literature on discrete distillation remains relatively sparse. Progress has largely relied on porting continuous primitives into categorical token spaces. This introduces severe structural challenges: the non-differentiability of token sampling, the lack of deterministic latent trajectories under masked corruption, and the factorization error inherent in single-step predictions.

To navigate these challenges, recent methods in both visual and language domains explore diverse adaptations. One prominent direction adapts distribution matching to discrete outputs by minimizing token-level divergences. Di[M]O performs on-policy token-level distribution matching with an auxiliary model initialized from the teacher, which approximates the student’s intermediate conditional distributions and provides gradients directly on generator logits, avoiding backpropagation through discrete sampling [60]. Soft-Di[M]O further relaxes discrete outputs into soft embeddings, enabling end-to-end differentiable refinements such as adversarial fine-tuning [61]. Alternative approaches mitigate product-factorization errors by parameterizing student transitions as mixtures of product models to capture dimensional correlations [17], or by iteratively rectifying source–target couplings to reduce conditional total correlation in discrete flows [57]. In the language domain, SDTT distills masked discrete diffusion language models by matching student predictions to teacher-generated multi-step denoising targets [12], while D-MMD generalizes continuous moment-matching distillation to discrete/categorical diffusion models [22].

Crucially, existing discrete distillation methods typically incur substantial computational overhead, either through online learnable auxiliary networks that effectively double training cost, or through multi-stage pipelines that fragment optimization into separate offline phases. Our framework sidesteps both issues by formulating distillation as a fixed-point matching problem, replacing trajectory-level imitation with local corrections derived from the student’s own drafts, requiring no additional trainable components beyond the student and remaining agnostic to the teacher’s masking schedule.

## 3 Method

We first review the discrete diffusion framework in Sec. 3.1, then present our fixed-point formulation that constructs training targets from the student’s own re-masked drafts in Sec. 3.2. The resulting residual is computed via a multi-bandwidth drift loss in a lifted continuous feature space, as detailed in Sec. 3.3. Finally, Sec. 3.4 describes the straight-through estimator that bridges the discrete bottleneck and enables an optional adversarial objective.

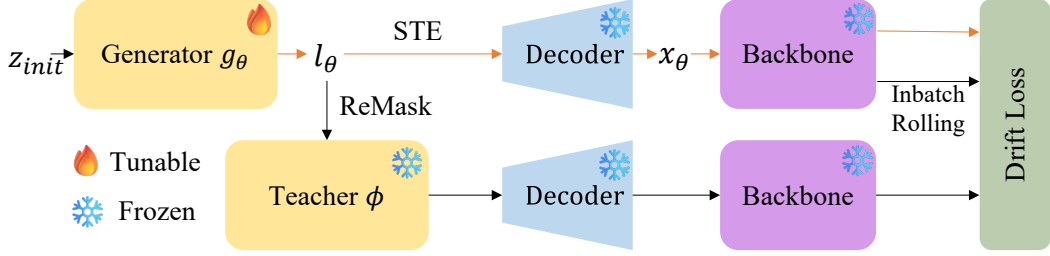


Figure 2: **Overview of the proposed distillation framework.** The student model processes a masked initialization  $z_{init}$  to output logits  $l_\theta$ . Via a Straight-Through Estimator (STE), these discrete outputs are decoded into a continuous image  $x_\theta$  and mapped to a feature space by a frozen backbone  $\Phi$ . Concurrently, the student’s token draft is partially re-masked ( $\mathcal{M}_r$ ) and refined by the frozen teacher. The decoded teacher features serve as positive targets, while cyclically shifted in-batch student features act as negatives to compute the drift loss  $\mathcal{L}_{drift}$ . An auxiliary GAN loss  $\mathcal{L}_{gan}$  is applied to  $x_\theta$  for enhanced perceptual quality. Black lines denote forward computation paths, while red lines highlight the differentiable gradient flow that safely bypasses the discrete bottleneck. The backbone and decoder share the same weights.

### 3.1 Preliminaries: Discrete Diffusion for Image Generation

Let  $x \in \mathbb{R}^{3 \times H \times W}$  be an image and let  $(\mathcal{E}, \mathcal{D})$  denote a frozen VQ encoder-decoder pair with codebook  $E \in \mathbb{R}^{K \times d}$ , where  $K$  is the codebook size and  $d$  the embedding dimension. The encoder maps an image to a length- $L$  sequence of discrete codes  $z = (z_1, \dots, z_L) \in \mathcal{V}^L$  with  $\mathcal{V} = \{1, \dots, K\}$ , and the decoder reconstructs an image via  $\mathcal{D}(E[z])$ . We write  $E[z] \in \mathbb{R}^{L \times d}$  for the row-wise codebook lookup. Text conditioning  $c$  is produced by a separate frozen text encoder.

**Forward masking process.** Discrete diffusion augments the token vocabulary with a special mask symbol  $[M] \notin \mathcal{V}$ , yielding  $\bar{\mathcal{V}} = \mathcal{V} \cup \{[M]\}$ . For a continuous timestep  $t \in [0, 1]$  and a monotonically increasing noise schedule  $\gamma : [0, 1] \rightarrow [0, 1]$ , each position is independently replaced with  $[M]$  with probability  $\gamma(t)$ :

$$q(z_t | z) = \prod_{i=1}^L [(1 - \gamma(t)) \delta_{z_t, i, z_i} + \gamma(t) \delta_{z_t, i, [M]}]. \quad (1)$$

**Reverse unmasking process.** A teacher network  $f_\phi : \bar{\mathcal{V}}^L \times \mathcal{C} \times [0, 1] \rightarrow \mathbb{R}^{L \times K}$  outputs per-position logits  $\ell = f_\phi(z_t, c, t)$ , which define a categorical distribution  $p_\phi(z_{0,i} = v | z_t, c, t) \propto \exp(\ell_{i,v})$ , where  $\mathcal{C}$  denotes the text conditioning space. The training objective minimizes the cross-entropy loss on the masked positions,

$$\mathcal{L}_\phi = \mathbb{E}_{t, z \sim p_{data}, z_t \sim q(\cdot | z)} \left[ - \sum_{i: z_{t,i}=[M]} \log p_\phi(z_i | z_t, c, t) \right]. \quad (2)$$

During inference, generation proceeds iteratively from a fully masked sequence  $z_T = ([M], \dots, [M])$ . At each of the  $T$  steps, the model predicts all masked positions, retains a top-confidence subset, and re-masks the remainder according to  $\gamma$ . We denote a single such teacher refinement step at mask ratio  $r$  by  $\mathcal{T}_\phi^r$ . After  $T$  steps, the final tokens  $\hat{z}$  are decoded to pixels via  $\hat{x} = \mathcal{D}(E[\hat{z}]; c)$ .

**Distillation.** To eliminate this iterative overhead, our distillation framework trains a single-step student  $g_\theta$  that directly maps a masked initialization to a high-quality sample, bypassing the teacher’s multi-step inference process. The following section details our approach.

### 3.2 Fixed-Point Iteration via Local Correction

The teacher’s reverse process is a sequence of refinements  $\mathcal{T}_\phi^{r_1} \circ \mathcal{T}_\phi^{r_2} \circ \dots$  that progressively reduce the masking level. A correctly distilled single-step student  $g_\theta$  should produce, in one forward pass, a sample  $\hat{z}$  that is already a *fixed point* of the teacher’s refinement operator: re-masking  $\hat{z}$  at any level  $r$  and applying  $\mathcal{T}_\phi^r$  should leave its distribution invariant. Writing  $p_\theta$  for the student’s marginal, this

requirement can be stated as

$$p_\theta = (\mathcal{T}_\phi^r \circ \mathcal{M}_r)_{\#} p_\theta, \quad \forall r \in (0, 1), \quad (3)$$

where  $\#$  denotes the pushforward measure.

Enforcing Eq. 3 directly as a global distributional constraint is intractable. Instead, we minimize the local correction residual. Although the teacher suffers from severe truncation error when generating in a single step from pure noise, its local refinement from intermediate noise levels remains faithful to its original training objective. Evaluating the teacher on the student’s partially re-masked draft therefore provides a valid descent direction toward the data manifold.

As shown in Fig. 2, we construct an end-to-end training pipeline. For each prompt  $c$ , we instantiate a nearly fully masked initialization  $z_{\text{init}}$  at a high mask ratio  $r_{\text{init}}$ , with the unmasked positions filled by random codebook entries. The student generates a full-sequence draft in one shot:

$$\ell_\theta = g_\theta(z_{\text{init}}, c), \quad \hat{z} \sim p_\theta(\cdot | z_{\text{init}}, c). \quad (4)$$

To compute the local correction signal, a single teacher refinement is performed at a randomly sampled intermediate mask ratio  $r \sim \pi$ :

$$\hat{z}_T = \mathcal{T}_\phi^r(\mathcal{M}_r(\hat{z}), c). \quad (5)$$

The pair  $(\hat{z}, \hat{z}_T)$  constitutes the empirical fixed-point residual. The training loss, detailed in Sec. 3.3, penalizes this discrepancy in a continuous feature space, pulling the student toward the teacher’s local refinement and enforcing the fixed-point condition across masking levels via the sampled  $r$ .

Unlike prior discrete distillation methods that require trajectory-level alignment or auxiliary learnable networks, our formulation optimizes a single fixed-point objective via local corrections derived from the student’s own drafts. Moreover, since both training and inference start from the same masked initialization  $z_{\text{init}}$ , the train- and test-time operating points coincide by construction.

### 3.3 Lifted Particle Optimization

To compute the fixed-point residual in a meaningful metric space, we lift the discrete tokens into a continuous feature space. Because the native output of a discrete diffusion model is a sequence of categorical tokens  $\hat{z} \in \mathcal{V}^L$ , no well-defined distance exists between token sequences. We bridge this gap by sequentially passing tokens through the codebook embedding  $E$ , the decoder  $\mathcal{D}$ , and a frozen feature backbone  $\Phi$ . For a student draft  $\hat{z}_i$  and its corresponding teacher refinement  $\hat{z}_{T,i}$ , the lifted spatial features are  $X_i = \Phi(\mathcal{D}(E[\hat{z}_i]; c_i))$  and  $Y_i = \Phi(\mathcal{D}(E[\hat{z}_{T,i}]; c_i))$ .

In this continuous space, following [11], we employ a multi-bandwidth drift objective to construct the optimization signal from these paired features. Within a mini-batch, the empirical drift vector  $V_h(X_i^f)$  at spatial position  $f$  and kernel bandwidth  $h$  is defined by an attractive force toward the teacher targets and a repulsive force from in-batch negative samples:

$$V_h(X_i^f) = \sum_j a_{ij}^+(h) (Y_j^f - X_i^f) - \sum_j a_{ij}^-(h) (X_{\sigma(j)}^f - X_i^f). \quad (6)$$

Here,  $\{X_{\sigma(j)}\}$  are cyclic in-batch shifts representing the student marginal, and  $a^\pm \propto \exp(-\|X_i^f - \cdot\|/h)$  are doubly-normalized softmax affinities derived from a Laplace kernel. The student is optimized to match the displaced target via a stop-gradient regression:

$$\mathcal{L}_{\text{drift}} = \sum_{h \in \mathcal{H}} \frac{1}{Z_h} \mathbb{E}_{i,f} \|X_i^f - \text{sg}(X_i^f + V_h(X_i^f))\|^2, \quad (7)$$

where  $\mathcal{H}$  is a set of bandwidths and  $Z_h$  is an RMS normalizer that equalizes gradient scales across bandwidths.

### 3.4 Differentiable Routing via the Discrete Bottleneck

The drift objective operates in continuous  $\hat{z}$  space, yet the student outputs discrete tokens  $\hat{z} \sim p_\theta$ . Standard continuous relaxations, such as probability-weighted soft embeddings  $\tilde{e}_i = \sum_v p_{\theta,iv} E_v$ ,

produce off-manifold vectors. Feeding such off-manifold inputs into the teacher network elicits out-of-distribution refinements and systematically biases the fixed-point target  $\hat{z}_T$ .

To maintain differentiability while preserving manifold consistency, we employ a hard-forward, soft-backward straight-through estimator (STE) [3]:

$$e_i^{\text{STE}} = E[\hat{z}_i] + \tilde{e}_i - \text{sg}(\tilde{e}_i). \quad (8)$$

In the forward pass,  $e_i^{\text{STE}} \equiv E[\hat{z}_i]$ , ensuring that both the decoder and the teacher network evaluate only valid codebook embeddings and preserving the integrity of the local correction signal. In the backward pass, gradients route through the soft embedding, yielding  $\partial e_i^{\text{STE}} / \partial \ell_{i,v} = \partial \tilde{e}_i / \partial \ell_{i,v}$ , which translates the continuous drift force from the feature space back to the student logits.

This differentiable pixel-to-logit pathway natively supports image-level adversarial supervision. We optionally augment the training with an unconditional GAN objective  $\mathcal{L}_{\text{gan}}$  applied to the decoded student images. Because the drift loss already enforces conditional and structural correspondence with the teacher targets, the unconditional discriminator serves solely to enhance high-frequency details and perceptual realism. The final training objective is:

$$\mathcal{L}_{\text{total}} = \mathcal{L}_{\text{drift}} + \lambda \mathcal{L}_{\text{gan}},$$

where  $\lambda$  is a hyperparameter balancing the adversarial penalty against the fixed-point correction.

## 4 Experiment

We evaluate Fixed-Point Distillation on both class-conditional and text-to-image generation, addressing three questions: 1) Can a single-step discrete generator match multi-step teacher quality without an auxiliary score network? 2) How critical are the straight-through estimator and the student-driven refinement source to the fixed-point formulation? 3) How should the lifted drift space be configured in terms of feature layers, spatial granularity, and kernel bandwidths?

### 4.1 Experimental Settings

**Datasets and Metrics.** We evaluate on both class-conditional and text-to-image generation. For class-conditional generation, we use ImageNet [10]; for text-to-image generation, we use a 400K-image subset of LAION [47]. Note that the drift loss requires only conditioning signals, i.e., class labels or text captions, to query the frozen teacher, while real images enter the pipeline solely through the unconditional discriminator. For class-conditional evaluation, we generate 50,000 images and report Fréchet Inception Distance [18], Inception Score [42], and Precision and Recall [25]. For text-to-image evaluation, we report results on the GenEval [15] benchmark.

**Implementation Details.** We initialize the student from pre-trained MaskGIT and MaskGen-L for class-conditional and text-to-image generation, respectively. The frozen feature backbone is DINOv3 ViT-B/16 [49], from which we extract multi-scale spatial features at blocks  $\{2, 5, 8, 11\}$  with drift bandwidths  $\mathcal{H} = \{0.02, 0.05, 0.2\}$ . Both the feature backbone and the VQ decoder remain frozen throughout training. All models are optimized with AdamW at a learning rate of  $1 \times 10^{-5}$ , using a batch size of 32 for MaskGIT and 64 for MaskGen-L.

We optionally incorporate a StyleGAN-XL [46] discriminator to enhance perceptual quality. The discriminator is unconditional and trained on real images only, ensuring that all conditional generation capability originates from the drift loss rather than from adversarial supervision.

**Baselines.** For class-conditional generation, we compare against the MaskGIT [4] teacher at varying inference steps, as well as recent discrete distillation methods: SDTT [12], di4c [17], ReDi [57], and DiMO [60]. For text-to-image generation, we compare against the MaskGen teacher, the discrete baseline DiMO [60], and a broad range of continuous distillation methods including InstaFlow [27], SiD-LSG [58], LCM [30], TDM [32], ADD [45], and DMD2 [55].

### 4.2 Main Results

We compare our method against existing approaches on text-to-image and class-conditional generation in Tab. 1 and Tab. 2, respectively. Both tables additionally report whether each distillation method requires an auxiliary score network, an online learnable network that approximates the score of the

Table 1: Comparison of various text-to-image generation models on the GenEval benchmark. The symbols  $\uparrow$  and  $\downarrow$  indicate that higher and lower scores are preferable, respectively. “#Model Params” is the inference parameter count.

Methods	Steps $\downarrow$	#Model Params	Aux. Score Net	GenEval $\uparrow$						
				Single	Two	Count.	Colors	Pos.	Color Attr.	Overall
<i>Foundation Models</i>										
LDM [39]	50	1.4B	-	0.92	0.29	0.23	0.70	0.02	0.05	0.37
DALLE 2 [37]	-	4.2B	-	0.94	0.66	0.49	0.77	0.10	0.19	0.52
SDXL [35]	50	2.6B	-	0.98	0.74	0.39	0.85	0.15	0.23	0.55
MaskGen [24]	16	0.6B	-	0.97	0.55	0.38	0.80	0.08	0.14	0.48
<i>Continuous Distillation</i>										
InstaFlow [27]	1	0.9B	$\times$	0.88	0.21	0.20	0.66	0.03	0.03	0.33
SiD-LSG [58]	1	0.9B	$\checkmark$	0.93	0.37	0.21	0.57	0.03	0.03	0.36
RG-LCM (HPS) [26]	2	0.9B	$\times$	0.97	0.54	0.35	0.82	0.07	0.14	0.48
TDM [32]	4	0.9B	$\checkmark$	0.99	0.57	0.49	0.78	0.09	0.09	0.50
SDXL-LCM [30]	1	2.6B	$\times$	0.75	0.11	0.14	0.59	0.01	0.03	0.27
SDXL-LCM [30]	4	2.6B	$\times$	0.99	0.57	0.39	0.86	0.09	0.18	0.51
SDXL-Turbo [45]	1	2.6B	$\times$	0.99	0.65	0.52	0.87	0.12	0.19	0.55
SDXL-DMD2 [55]	1	2.6B	$\checkmark$	0.99	0.68	0.48	0.90	0.08	0.19	0.55
<i>Discrete Distillation</i>										
MaskGen-DiMO [60]	1	0.6B	$\checkmark$	0.93	0.39	0.35	0.74	0.07	0.08	0.42
MaskGen-FPD (Ours)	1	0.6B	$\times$	0.96	0.36	0.43	0.76	0.09	0.09	0.45

Table 2: Quantitative results on class-conditional ImageNet-256 with MaskGit teacher.

Method	Steps $\downarrow$	Aux. Score Net	FID $\downarrow$	IS $\uparrow$	Prec. $\uparrow$	Rec. $\uparrow$
MaskGit [4]	16	-	6.60	224	0.83	0.40
MaskGit [4]	8	-	6.66	222	0.83	0.40
MaskGit [4]	4	-	10.73	192	0.75	0.31
MaskGit [4]	2	-	91.35	13	0.18	0.16
<i>Discrete Distillation</i>						
SDTT [12]	4	$\times$	8.97	205	0.88	0.41
SDTT [12]	1	$\times$	90.40	14	0.31	0.13
di4c [17]	4	$\times$	6.79	209	-	-
di4c-d [17]	4	$\times$	6.57	214	-	-
ReDi <sup>1</sup> [57]	4	$\times$	7.58	228	0.87	0.46
ReDi <sup>2</sup> [57]	4	$\times$	7.86	240	0.87	0.44
ReDi <sup>3</sup> -distill [57]	1	$\times$	11.68	182	0.83	0.44
DiMO [60]	1	$\checkmark$	6.91	214	0.83	0.38
FPD (Ours)	1	$\times$	6.90	215	0.81	0.35

student’s output distribution and is updated jointly with the student. Such a network is typically the same size as the teacher, effectively doubling training compute.

**Text-to-Image Generation.** Tab. 1 demonstrates the efficacy of our approach in achieving high-quality single-step generation without the severe degradation typical of extreme distillation. On the GenEval text-to-image benchmark, the distilled MaskGen-FPD achieves an overall score of 0.45 in a single step using an efficient 0.6B parameter budget. This outperforms the competing one-step discrete baseline MaskGen-DiMO, which scores 0.42. Notably, our method yields significant gains in the Counting metric, reaching 0.43 compared to DiMO’s 0.35. Furthermore, it successfully retains roughly 94% of the overall performance of the 16-step MaskGen teacher, which scores 0.48. Fig. 1 and Fig. 3 visually demonstrate the effectiveness of our method, whereas one-step generation directly from the teacher collapses entirely.

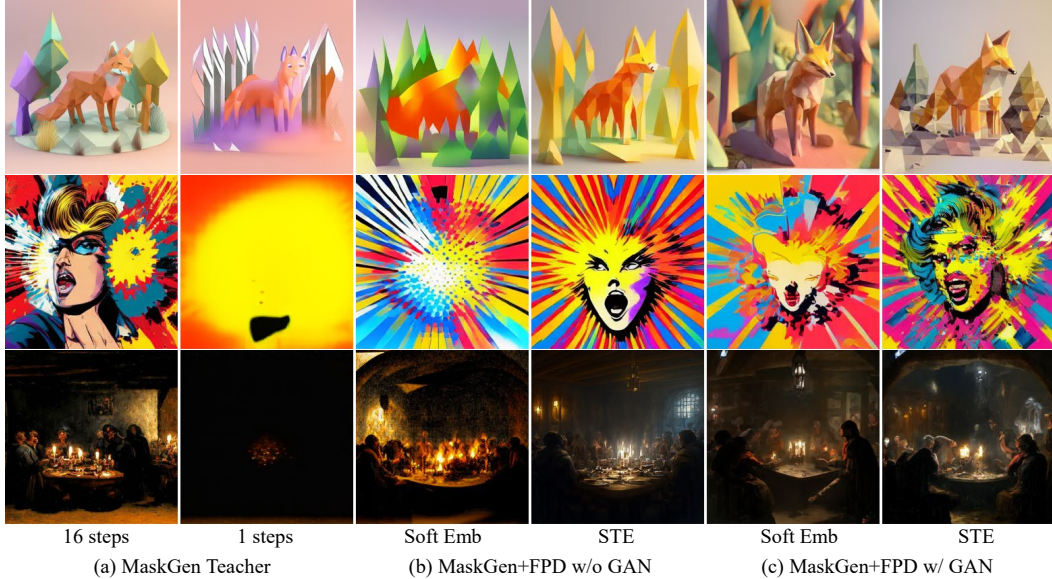


Figure 3: Training strategy comparisons. We compare the multi-step teacher baselines with our single-step FPD variants, demonstrating the superiority of the Straight-Through Estimator in preserving structural integrity, and the perceptual enhancements introduced by the auxiliary GAN loss.

Table 3: Ablations on gradient routing and teacher refinement, evaluated on GenEval. (a) Impact of the discrete bottleneck strategy and the optional adversarial loss. *Soft Emb.* computes a probability-weighted codebook mixture; *STE* uses hard-sampled tokens in the forward pass. (b) Refinement source for the teacher target: *Student* re-masks the student’s own draft; *Random* initialises all positions randomly.

(a) Gradient Routing and Adversarial Loss			(b) Refinement Source	
Estimator	w/ $\mathcal{L}_{\text{gan}}$	Overall $\uparrow$	Draft Source	Overall $\uparrow$
Soft Emb.		0.38	Random	0.22
Soft Emb.	✓	0.42	Student	<b>0.43</b>
STE		0.43		
STE	✓	<b>0.45</b>		

**Class-Conditional Generation.** This robustness extends to class-conditional ImageNet-256 generation, as detailed in Tab. 2. Our method establishes a highly competitive one-step FID of 6.90 and an Inception Score of 215. While prior discrete distillation approaches fail severely at a single step, such as SDTT degrading to an FID of 90.40, or struggle to close the quality gap, as seen with ReDi<sup>3</sup>-distill at 11.68, our single-step output rivals the quality of multi-step samplers. Specifically, it eclipses the 4-step ReDi<sup>1</sup>, which yields an FID of 7.58, and performs on par with the recent one-step DiMO baseline at 6.91, while bridging the performance gap toward the 16-step MaskGit teacher, which holds an FID of 6.60. These empirical results confirm that the fixed-point formulation successfully condenses the iterative generation process into a single evaluation while strictly preserving visual fidelity and structural alignment.

### 4.3 Ablation Studies

**Gradient Routing and Adversarial Supervision.** Tab. 3a and Fig. 3 evaluate the gradient routing strategy alongside the optional adversarial loss. Replacing the soft embedding path with the Straight-Through Estimator improves the GenEval score from 0.38 to 0.43, confirming that preserving exact hard sampling during the forward pass prevents out-of-distribution teacher evaluations and maintains train–test manifold consistency. As illustrated in Fig. 3, soft embeddings introduce visible artifacts

Table 4: Feature space ablations on GenEval. (a) Representation space and kernel bandwidths for the drift objective. (b) Layer selection and spatial granularity of the frozen feature backbone (DINOv3-B, 12 layers). *Patch Grid* indicates whether features are kept on a  $4\times 4$  spatial grid or globally average-pooled into a single vector.

(a) Drift Space and Kernel Bandwidths			(b) Backbone Layer Selection		
Space	Bandwidths	Overall $\uparrow$	Blocks	Patch Grid	Overall $\uparrow$
Pixel	{0.02, 0.05, 0.2}	0.21	{2,5,8,11}		0.34
Feature	{0.05}	0.41	{2,5}	✓	0.35
Feature	{0.02, 0.05, 0.2}	<b>0.43</b>	{8,11}	✓	0.42
			{2,5,8,11}	✓	<b>0.43</b>

and structural distortions, since the teacher and decoder receive off-manifold inputs that deviate from their training distribution. This result also shows that the fixed-point framework is effective on its own, establishing a strong generative baseline without any adversarial supervision. Adding  $\mathcal{L}_{\text{gan}}$  further improves both routing paths, with the STE combination reaching the highest score of 0.45. The unconditional discriminator primarily enhances high-frequency details and perceptual sharpness, acting as a complementary booster rather than the primary source of semantic alignment.

**Student-Driven Teacher Refinement.** Tab. 3b validates the fixed-point formulation by comparing the refinement source. When the teacher refines a random token sequence instead of the student’s own draft, performance collapses from 0.43 to 0.22. This confirms that the teacher’s value lies in providing localized, state-dependent corrections to the student’s current output rather than acting as a standalone generator. Intuitively, the student’s draft already captures coarse structure from its conditioning signal; the teacher then sharpens this structure through targeted refinement of the re-masked positions. When this coupling is removed, the teacher must reconstruct the entire sequence from scratch, and the resulting drift vectors bear no relation to the student’s generative state, leaving the optimization without a coherent descent direction.

**Lifted Drift Space.** Tab. 4a and Tab. 4b validate the configuration of the drift objective. Computing the loss in raw pixel space yields only 0.21, as pixel-level distances are dominated by low-level variations and fail to capture the semantic structure needed to guide distillation. Lifting tokens into a pre-trained feature space is therefore essential. Within that space, the choice of layers and spatial granularity both matter. Relying on global average pooling discards spatial correspondence between the student and teacher outputs, while using only shallow layers provides features that lack sufficient semantic abstraction. A full multi-layer spatial configuration over blocks  $\{2, 5, 8, 11\}$  with a  $4\times 4$  patch grid captures both mid-level structure and high-level semantics, reaching 0.43. Finally, a multi-scale bandwidth set  $\mathcal{H}$  outperforms a single bandwidth by allowing the drift kernel to simultaneously enforce coarse global alignment at large  $h$  and fine-grained local discrimination at small  $h$ .

## 5 Conclusion

We presented Fixed-Point Distillation, a framework enabling high-fidelity single-step generation for discrete diffusion models. By formulating distillation as a fixed-point matching problem, we lift discrete tokens into a continuous feature space, allowing for efficient particle optimization via a drift loss without auxiliary score networks. To resolve the discrete bottleneck, we employed a straight-through estimator that ensures manifold consistency for the teacher evaluations while routing structured continuous gradients back to the student logits. This differentiable pathway additionally supports unconditional adversarial supervision to enhance perceptual realism. Experiments on class- and text-condition generation benchmarks achieve competitive results compared to existing methods, condensing the iterative sampling process into a single evaluation while preserving structural alignment and visual quality.

## References

- [1] Niket Agarwal, Arslan Ali, Maciej Bala, Yogesh Balaji, Erik Barker, Tiffany Cai, Prithvijit Chattopadhyay, Yongxin Chen, Yin Cui, Yifan Ding, et al. Cosmos world foundation model platform for physical ai. *arXiv preprint arXiv:2501.03575*, 2025.
- [2] Jacob Austin, Daniel D Johnson, Jonathan Ho, Daniel Tarlow, and Rianne Van Den Berg. Structured denoising diffusion models in discrete state-spaces. *Advances in neural information processing systems*, 34:17981–17993, 2021.
- [3] Yoshua Bengio, Nicholas Léonard, and Aaron Courville. Estimating or propagating gradients through stochastic neurons for conditional computation. *arXiv preprint arXiv:1308.3432*, 2013.
- [4] Victor Besnier and Mickael Chen. A pytorch reproduction of masked generative image transformer. *arXiv preprint arXiv:2310.14400*, 2023.
- [5] Sam Bond-Taylor, Peter Hesse, Hiroshi Sasaki, Toby P Breckon, and Chris G Willcocks. Unleashing transformers: Parallel token prediction with discrete absorbing diffusion for fast high-resolution image generation from vector-quantized codes. In *European Conference on Computer Vision*, pages 170–188. Springer, 2022.
- [6] Tim Brooks, Aleksander Holynski, and Alexei A Efros. Instructpix2pix: Learning to follow image editing instructions. In *Proceedings of the IEEE/CVF conference on computer vision and pattern recognition*, pages 18392–18402, 2023.
- [7] Jake Bruce, Michael D Dennis, Ashley Edwards, Jack Parker-Holder, Yuge Shi, Edward Hughes, Matthew Lai, Aditi Mavalankar, Richie Steigerwald, Chris Apps, et al. Genie: Generative interactive environments. In *Forty-first International Conference on Machine Learning*, 2024.
- [8] Andrew Campbell, Joe Benton, Valentin De Bortoli, Thomas Rainforth, George Deligiannidis, and Arnaud Doucet. A continuous time framework for discrete denoising models. *Advances in Neural Information Processing Systems*, 35:28266–28279, 2022.
- [9] Huiwen Chang, Han Zhang, Lu Jiang, Ce Liu, and William T Freeman. Maskgit: Masked generative image transformer. In *Proceedings of the IEEE/CVF conference on computer vision and pattern recognition*, pages 11315–11325, 2022.
- [10] Jia Deng, Wei Dong, Richard Socher, Li-Jia Li, Kai Li, and Li Fei-Fei. Imagenet: A large-scale hierarchical image database. In *2009 IEEE conference on computer vision and pattern recognition*, pages 248–255. Ieee, 2009.
- [11] Mingyang Deng, He Li, Tianhong Li, Yilun Du, and Kaiming He. Generative modeling via drifting. *arXiv preprint arXiv:2602.04770*, 2026.
- [12] Justin Deschenaux and Caglar Gulcehre. Beyond autoregression: Fast llms via self-distillation through time. *arXiv preprint arXiv:2410.21035*, 2024.
- [13] Patrick Esser, Sumith Kulal, Andreas Blattmann, Rahim Entezari, Jonas Müller, Harry Saini, Yam Levi, Dominik Lorenz, Axel Sauer, Frederic Boesel, et al. Scaling rectified flow transformers for high-resolution image synthesis. In *Forty-first international conference on machine learning*, 2024.
- [14] Zhengyang Geng, Mingyang Deng, Xingjian Bai, J Zico Kolter, and Kaiming He. Mean flows for one-step generative modeling. *arXiv preprint arXiv:2505.13447*, 2025.
- [15] Dhruva Ghosh, Hannaneh Hajishirzi, and Ludwig Schmidt. Geneval: An object-focused framework for evaluating text-to-image alignment. *Advances in Neural Information Processing Systems*, 36:52132–52152, 2023.
- [16] Shuyang Gu, Dong Chen, Jianmin Bao, Fang Wen, Bo Zhang, Dongdong Chen, Lu Yuan, and Baining Guo. Vector quantized diffusion model for text-to-image synthesis. In *Proceedings of the IEEE/CVF conference on computer vision and pattern recognition*, pages 10696–10706, 2022.
- [17] Satoshi Hayakawa, Yuhta Takida, Masaaki Imaizumi, Hiromi Wakaki, and Yuki Mitsufuji. Distillation of discrete diffusion through dimensional correlations. *arXiv preprint arXiv:2410.08709*, 2024.
- [18] Martin Heusel, Hubert Ramsauer, Thomas Unterthiner, Bernhard Nessler, and Sepp Hochreiter. Gans trained by a two time-scale update rule converge to a local nash equilibrium. *Advances in neural information processing systems*, 30, 2017.
- [19] Jonathan Ho, Ajay Jain, and Pieter Abbeel. Denoising diffusion probabilistic models. *Advances in neural information processing systems*, 33:6840–6851, 2020.
- [20] Jonathan Ho, Tim Salimans, Alexey Gritsenko, William Chan, Mohammad Norouzi, and David J Fleet. Video diffusion models. *Advances in neural information processing systems*, 35:8633–8646, 2022.
- [21] Wenyi Hong, Ming Ding, Wendi Zheng, Xinghan Liu, and Jie Tang. Cogvideo: Large-scale pretraining for text-to-video generation via transformers. *arXiv preprint arXiv:2205.15868*, 2022.
- [22] Emiel Hoogeboom, David Ruhe, Jonathan Heek, Thomas Mensink, and Tim Salimans. Beyond single tokens: Distilling discrete diffusion models via discrete mmd. *arXiv preprint arXiv:2603.20155*, 2026.
- [23] Minghui Hu, Chuanxia Zheng, Heliang Zheng, Tat-Jen Cham, Chaoyue Wang, Zuopeng Yang, Dacheng Tao, and Ponnuthurai N Suganthan. Unified discrete diffusion for simultaneous vision-language generation. *arXiv preprint arXiv:2211.14842*, 2022.

- [24] Dongwon Kim, Ju He, Qihang Yu, Chenglin Yang, Xiaohui Shen, Suha Kwak, and Liang-Chieh Chen. Democratizing text-to-image masked generative models with compact text-aware one-dimensional tokens. In *ICCV*, 2025.
- [25] Tuomas Kynkäänniemi, Tero Karras, Samuli Laine, Jaakko Lehtinen, and Timo Aila. Improved precision and recall metric for assessing generative models. *Advances in neural information processing systems*, 32, 2019.
- [26] Jiachen Li, Weixi Feng, Wenhui Chen, and William Yang Wang. Reward guided latent consistency distillation. *arXiv preprint arXiv:2403.11027*, 2024.
- [27] Xingchao Liu, Xiwen Zhang, Jianzhu Ma, Jian Peng, et al. InstafLOW: One step is enough for high-quality diffusion-based text-to-image generation. In *The Twelfth International Conference on Learning Representations*, 2023.
- [28] Aaron Lou, Chenlin Meng, and Stefano Ermon. Discrete diffusion modeling by estimating the ratios of the data distribution. *arXiv preprint arXiv:2310.16834*, 2023.
- [29] Cheng Lu and Yang Song. Simplifying, stabilizing and scaling continuous-time consistency models. *arXiv preprint arXiv:2410.11081*, 2024.
- [30] Simian Luo, Yiqin Tan, Longbo Huang, Jian Li, and Hang Zhao. Latent consistency models: Synthesizing high-resolution images with few-step inference. *arXiv preprint arXiv:2310.04378*, 2023.
- [31] Weijian Luo, Tianyang Hu, Shifeng Zhang, Jiacheng Sun, Zhenguo Li, and Zhihua Zhang. Diff-instruct: A universal approach for transferring knowledge from pre-trained diffusion models. *Advances in Neural Information Processing Systems*, 36:76525–76546, 2023.
- [32] Yihong Luo, Tianyang Hu, Jiacheng Sun, Yujun Cai, and Jing Tang. Learning few-step diffusion models by trajectory distribution matching. In *Proceedings of the IEEE/CVF International Conference on Computer Vision*, pages 17719–17728, 2025.
- [33] Chenlin Meng, Yutong He, Yang Song, Jiaming Song, Jiajun Wu, Jun-Yan Zhu, and Stefano Ermon. Sdedit: Guided image synthesis and editing with stochastic differential equations. *arXiv preprint arXiv:2108.01073*, 2021.
- [34] Alex Nichol, Prafulla Dhariwal, Aditya Ramesh, Pranav Shyam, Pamela Mishkin, Bob McGrew, Ilya Sutskever, and Mark Chen. Glide: Towards photorealistic image generation and editing with text-guided diffusion models. *arXiv preprint arXiv:2112.10741*, 2021.
- [35] Dustin Podell, Zion English, Kyle Lacey, Andreas Blattmann, Tim Dockhorn, Jonas Müller, Joe Penna, and Robin Rombach. Sdxl: Improving latent diffusion models for high-resolution image synthesis. *arXiv preprint arXiv:2307.01952*, 2023.
- [36] Ben Poole, Ajay Jain, Jonathan T Barron, and Ben Mildenhall. Dreamfusion: Text-to-3d using 2d diffusion. *arXiv preprint arXiv:2209.14988*, 2022.
- [37] Aditya Ramesh, Prafulla Dhariwal, Alex Nichol, Casey Chu, and Mark Chen. Hierarchical text-conditional image generation with clip latents. *arXiv preprint arXiv:2204.06125*, 2022.
- [38] Aditya Ramesh, Mikhail Pavlov, Gabriel Goh, Scott Gray, Chelsea Voss, Alec Radford, Mark Chen, and Ilya Sutskever. Zero-shot text-to-image generation. In *International conference on machine learning*, pages 8821–8831. Pmlr, 2021.
- [39] Robin Rombach, Andreas Blattmann, Dominik Lorenz, Patrick Esser, and Björn Ommer. High-resolution image synthesis with latent diffusion models. In *Proceedings of the IEEE/CVF conference on computer vision and pattern recognition*, pages 10684–10695, 2022.
- [40] Chitwan Saharia, William Chan, Saurabh Saxena, Lala Li, Jay Whang, Emily L Denton, Kamyar Ghasemipour, Raphael Gontijo Lopes, Burcu Karagol Ayan, Tim Salimans, et al. Photorealistic text-to-image diffusion models with deep language understanding. *Advances in neural information processing systems*, 35:36479–36494, 2022.
- [41] Subham S Sahoo, Marianne Arriola, Yair Schiff, Aaron Gokaslan, Edgar Marroquin, Justin T Chiu, Alexander Rush, and Volodymyr Kuleshov. Simple and effective masked diffusion language models. *Advances in Neural Information Processing Systems*, 37:130136–130184, 2024.
- [42] Tim Salimans, Ian Goodfellow, Wojciech Zaremba, Vicki Cheung, Alec Radford, and Xi Chen. Improved techniques for training gans. *Advances in neural information processing systems*, 29, 2016.
- [43] Tim Salimans and Jonathan Ho. Progressive distillation for fast sampling of diffusion models. *arXiv preprint arXiv:2202.00512*, 2022.
- [44] Axel Sauer, Frederic Boesel, Tim Dockhorn, Andreas Blattmann, Patrick Esser, and Robin Rombach. Fast high-resolution image synthesis with latent adversarial diffusion distillation. In *SIGGRAPH Asia 2024 Conference Papers*, pages 1–11, 2024.
- [45] Axel Sauer, Dominik Lorenz, Andreas Blattmann, and Robin Rombach. Adversarial diffusion distillation. In *European Conference on Computer Vision*, pages 87–103. Springer, 2024.
- [46] Axel Sauer, Katja Schwarz, and Andreas Geiger. Stylegan-xl: Scaling stylegan to large diverse datasets. In *ACM SIGGRAPH 2022 conference proceedings*, pages 1–10, 2022.
- [47] Christoph Schuhmann and Romain Beaumont. Laion-aesthetics. *LAION. AI*, 4, 2022.

- [48] Jiaxin Shi, Kehang Han, Zhe Wang, Arnaud Doucet, and Michalis Titsias. Simplified and generalized masked diffusion for discrete data. *Advances in neural information processing systems*, 37:103131–103167, 2024.
- [49] Oriane Siméoni, Huy V Vo, Maximilian Seitzer, Federico Baldassarre, Maxime Oquab, Cijo Jose, Vasil Khalidov, Marc Szafraniec, Seungeun Yi, Michaël Ramamonjisoa, et al. Dinov3. *arXiv preprint arXiv:2508.10104*, 2025.
- [50] Uriel Singer, Adam Polyak, Thomas Hayes, Xi Yin, Jie An, Songyang Zhang, Qiyuan Hu, Harry Yang, Oron Ashual, Oran Gafni, et al. Make-a-video: Text-to-video generation without text-video data. *arXiv preprint arXiv:2209.14792*, 2022.
- [51] Yang Song, Prafulla Dhariwal, Mark Chen, and Ilya Sutskever. Consistency models. In *International Conference on Machine Learning*, pages 32211–32252, 2023.
- [52] Yang Song, Jascha Sohl-Dickstein, Diederik P Kingma, Abhishek Kumar, Stefano Ermon, and Ben Poole. Score-based generative modeling through stochastic differential equations. *arXiv preprint arXiv:2011.13456*, 2020.
- [53] Haoran Sun, Lijun Yu, Bo Dai, Dale Schuurmans, and Hanjun Dai. Score-based continuous-time discrete diffusion models. *arXiv preprint arXiv:2211.16750*, 2022.
- [54] Wilson Yan, Yunzhi Zhang, Pieter Abbeel, and Aravind Srinivas. Videogpt: Video generation using vq-vae and transformers. *arXiv preprint arXiv:2104.10157*, 2021.
- [55] Tianwei Yin, Michaël Gharbi, Taesung Park, Richard Zhang, Eli Shechtman, Fredo Durand, and William T Freeman. Improved distribution matching distillation for fast image synthesis. *Advances in neural information processing systems*, 37:47455–47487, 2024.
- [56] Tianwei Yin, Michaël Gharbi, Richard Zhang, Eli Shechtman, Fredo Durand, William T Freeman, and Taesung Park. One-step diffusion with distribution matching distillation. In *Proceedings of the IEEE/CVF conference on computer vision and pattern recognition*, pages 6613–6623, 2024.
- [57] Jaehoon Yoo, Wonjung Kim, and Seunghoon Hong. Redi: Rectified discrete flow. *arXiv preprint arXiv:2507.15897*, 2025.
- [58] Mingyuan Zhou, Zhendong Wang, Huangjie Zheng, and Hai Huang. Long and short guidance in score identity distillation for one-step text-to-image generation. *arXiv preprint arXiv:2406.01561*, 3, 2024.
- [59] Mingyuan Zhou, Huangjie Zheng, Zhendong Wang, Mingzhang Yin, and Hai Huang. Score identity distillation: Exponentially fast distillation of pretrained diffusion models for one-step generation. In *Forty-first International Conference on Machine Learning*, 2024.
- [60] Yuanzhi Zhu, Xi Wang, Stéphane Lathuilière, and Vicky Kalogeiton. Di [m] o: Distilling masked diffusion models into one-step generator. In *Proceedings of the IEEE/CVF International Conference on Computer Vision*, pages 18606–18618, 2025.
- [61] Yuanzhi Zhu, Xi Wang, Stéphane Lathuilière, and Vicky Kalogeiton. Soft-di [m] o: Improving one-step discrete image generation with soft embeddings. *arXiv preprint arXiv:2509.22925*, 2025.